PHYSICAL REVIEW B VOLUME 25, NUMBER 2 15 JANUARY 1982

Structures of oxygen-covered Ni(110) surfaces

S. Masuda, M. Nishijima, Y. Sakisaka, and M. Onchi
Department of Chemistry, Faculty of Science, Kyoto University, Kyoto, Japan
(Received 6 April 1981)

The structures of oxygen-covered Ni(110) surfaces have been studied at 300 K by the *in situ* combination of low-energy electron diffraction (LEED), high-resolution electron-energy-loss spectroscopy, Auger electron spectroscopy, and work-function-change measurement. The electron-energy-loss peaks due to the excitation of the nickel-oxygen stretching vibration have been observed at 480, 380, and 444 cm^{-1}. The 480-cm^{-1} peak is associated with the oxygen atoms in the short-bridge sites of the unreconstructed Ni(110) surface, the 380-cm^{-1} peak with the oxygen atoms which lie in the bridge sites of the Ni[001] rows of the reconstructed surface, and the 444-cm^{-1} peak with the nickel oxide patches. It is proposed, when the LEED (2×1) pattern is seen, that two structures, i.e., the unreconstructed and reconstructed (2×1)-O structures, are formed. The structures of the "initial"-(3×1)-O, (3×1)-O, (9×4) and disordered-nickel-oxide surfaces are discussed. Experimental results and discussion on the "Ni(110) (2×1)-O" surfaces produced by high-temperature heating are included.

I. INTRODUCTION

Information on the surface structure, i.e., the geometrical location of atoms on a solid surface, is of great importance in the understanding of surface properties and processes. The structures of clean and oxygen-covered Ni(110) surfaces at 300 K have been studied in some detail using low-energy-electron diffraction (LEED) by a number of investigators.[1–7] For the Ni(110) clean surface, the LEED (1×1) pattern is observed, indicating the existence of a laterally unreconstructed surface. By the exposure of the clean surface to oxygen, a series of LEED patterns is seen, in order of appearance "initial" (3×1), (2×1), (3×1), (9×4), and disordered nickel oxide. The initial-(3×1) pattern has been reported as strong and reproducible,[4,5,7] as seen only with difficulty,[6] or as not observed at all.[1–3] For the (2×1)-O structure, the reconstruction model and the simple-addition model have been proposed, respectively, by Germer *et al.*[1,3,4] and Demuth *et al.*[8,9] According to the reconstruction model, the Ni(110) substrate is reconstructed such that every other Ni[001] row is absent and that the oxygen atoms occupy the positions of the absent nickel atoms. Verheij *et al.*[10,11] have recently proposed, from the study using low-energy ion scattering (at 523 K), that the oxygen atoms lie in or close to the Ni[001] rows of the reconstructed nickel substrate. According to the simple-addition model deduced from the LEED dynamical calculation, the oxygen atoms are located in the short-bridge sites of the unreconstructed Ni(110) substrate. For the initial-(3×1)-O and (3×1)-O structures, Germer *et al.*[1,3,4] have proposed the reconstruction models. For the (9×4) structure, May and Germer[5] have proposed a two-dimensional pseudo-oxide model.

Experimentally, the "Ni(110) (2×1)-O" surface, as defined by the observation of the (2×1) pattern using LEED, can be produced by (1) room-temperature adsorption of oxygen on the Ni(110) clean surface,[1–3,5,7,12] (2) room-temperature adsorption of oxygen, followed by high-tempreature heating,[1–3,5] and (3) exposure of the Ni(110) clean surface to a large amount of oxygen, followed by high-temperature heating.[1,2,5,13] The question arises as to how these surfaces differ. This problem has been studied using LEED,[1–3,5,7] Rutherford backscattering,[13] etc.

In the present investigation, the structures of oxygen-covered Ni(110) surfaces produced at 300 K and the Ni(110) (2×1)-O surfaces produced by high-temperature heating have been studied using LEED, high-resolution electron-energy-loss spectroscopy (HRELS), Auger electron spectroscopy (AES), and work-function-change measurement ($\Delta\phi$). HRELS is a relatively new technique which yields direct information on the geometry and chemical state of adsorbates.[14] HRELS and LEED give complementary information on the surface structure: HRELS yields information on the local

structure, whereas LEED yields information on the long-range periodic structure of the surface. New models on the structures of oxygen-covered Ni(110) surfaces are proposed.

II. EXPERIMENTAL

The experiments were performed using an ultrahigh vacuum system with the base pressure of $\sim 1\times 10^{-10}$ Torr, by the *in situ* combined techniques of LEED, HRELS, AES, $\Delta\phi$, and mass spectroscopy. The high-resolution electron spectrometer which has been constructed by the authors for the present study consists of a monochromator and an energy analyzer, both of 127° cylindrical deflector type. For the HRELS measurements, the primary electron energy E_p of 1.9 eV and the incidence angle α of 60° with respect to the surface normal were used. The elastic peak in the specular reflection beam had the maximum intensity of $\sim 10^5$ counts/s (for a clean surface) and the full width at half maximum (FWHM) of ~ 65 cm^{-1}. The energy-loss region which has been measured extends from 0 up to 2500 cm^{-1}. The work-function change was determined using the retarding-field diode technique. The experimental error in the determination was $\sim \pm 0.02$ eV. The Ni(110) sample (Metals Research Corp.) used was of 99.999% purity and of 6 mm diam$\times$2 mm thickness. The clean Ni(110) surface, having the $p(1\times 1)$ LEED pattern, was carefully prepared by the standard technique (Ar^+-ion bombardment—annealing—oxidation—flashing cycles). No impurities were observed on the clean surface thus prepared within the detection limit of AES (using the LEED optics). The Auger peak-height ratio, H(noise)/H(Ni $L_{2,3}VV$), was less than 0.01, and the residual carbon, if any, was estimated to be less than 0.02 monolayer. Sample temperature was measured with a chromel-alumel thermocouple attached to the sample edge. Error in the measurement was estimated to be less than $\sim \pm 10$ K. Molecular oxygen was admitted into the vacuum chamber at $5\times 10^{-8}-5\times 10^{-7}$ Torr through a variable-leak valve. The oxygen pressure was monitored using the nude-type Bayard-Alpert ion gauge and calibrated by the gauge-sensitivity factor of oxygen (0.8 relative to nitrogen).[15] The oxgyen exposure was estimated by $\int p\,dt$ (p is the oxygen pressure, t is the time). Details of the experimental apparatus and techniques have been described in our previous paper.[16]

III. RESULTS

The LEED, HRELS, AES, and $\Delta\phi$ results are given below. The experimental results by the four techniques can be correlated with each other using a common parameter, the oxygen exposure. The four measurements were made *in situ*, but not simultaneously; however, the correlation of the experimental results was confirmed by many experiments. The reproducibility of the data has been confirmed. The oxygen exposures given in the data are understood to be the typical values measured.

A. LEED

As the Ni(110) clean surface was exposed to oxygen at 300 K, the following progression of LEED patterns was observed: (2×1), (3×1), (9×4), and the disordered nickel oxide. It is noted that the observed (9×4) pattern has been comparatively poor. The LEED streaks in the [110]Az were observed prior to the (2×1) pattern, and between the (2×1) and (3×1) patterns. The initial-(3×1) pattern was seen only with difficulty. The oxygen exposures required for the well-developed (2×1), (3×1), and (9×4) patterns were $\sim 0.8-1.2$, $3.4-4$, and $12-15$ langmuirs (L), respectively ($1\text{L}=10^{-6}$ Torr s); for the LEED streaks $\sim 0.2-0.4$ L and $\sim 2.5-3.3$ L; for the initial-(3×1) ~ 0.3 L. For the oxygen exposure of more than ~ 30 L, the diffuse Ni(110) substrate spots with a bright background attributed to the formation of the disordered-nickel-oxide structure were observed. The experimental results are summarized in Fig. 3 (Sec. III C). Our LEED results including the oxygen exposures required for the observation of the various LEED patterns are in reasonable agreement with those which have been reported by other investigators.[1–7] The LEED streaks have been studied in detail by Germer *et al.*[4]

B. HRELS

In Fig. 1 are shown the HRELS spectra, in the specular mode, at 300 K of oxygen-covered Ni(110) surfaces. The loss-peak intensities are normalized by their respective elastic peak intensities, and the results are presented such that all spectra are related to the same elastic peak. For the small oxygen exposure of less than ~ 0.15 L, a single loss peak at 480 cm^{-1} with the FWHM of ~ 80 cm^{-1} was

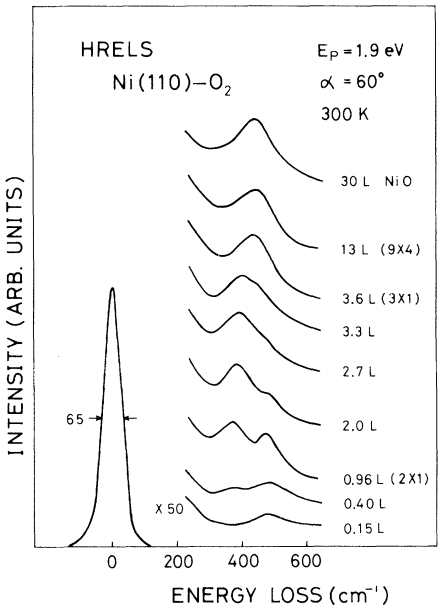

FIG. 1. Electron-energy-loss spectra, in the specular reflection mode, at 300 K, of oxygen-covered Ni(110) surfaces. The amounts of oxygen exposure and the observed LEED patterns are included.

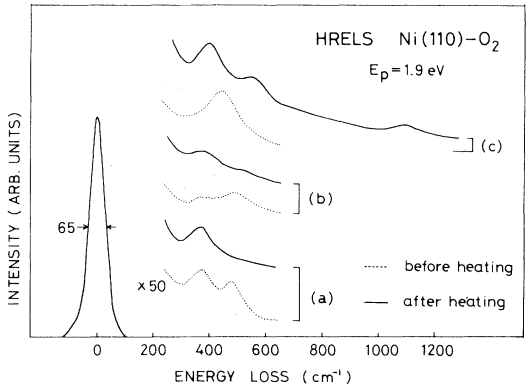

FIG. 2. Electron-energy-loss spectra of oxygen-covered Ni(110) surfaces. (a) Dotted curve, Ni(110) surface exposed to 0.96-L oxygen at 300 K; solid curve, after heating at 540 K for 1 min. (b) Dotted curve, Ni(110) surface exposed to 0.4-L oxygen at 300 K; solid curve, after heating at 630 K for 1 min. (c) Dotted curve, Ni(110) surface exposed to 30-L oxygen at 300 K; solid curve, after heating at 770 K for 1 min.

observed. The loss value was reproducible to within ± 12 cm^{-1}. With increasing oxygen exposure up to 0.4 L, the intensity of the 480 cm^{-1} peak was increased and, additionally, a new peak was observed at the loss energy of 380 cm^{-1}. As the oxygen exposure was increased to $\sim 0.8-1.2$ L [corresponding to the (2×1) pattern], two loss peaks at 380 and 480 cm^{-1} were observed with relatively large intensity. The intensity of the 480-cm^{-1} peak was decreased substantially for 2-L oxygen exposure, and the 480-cm^{-1} peak vanished for ~ 3.3 L. The 380-cm^{-1} peak was shifted monotonically towards higher energy for the oxygen exposure from 0.4 to 3.3 L, 384 cm^{-1} for 2-L oxygen exposure, and 400 cm^{-1} for 3.3 L. Furthermore, in this exposure region, the intensity of the 380-cm^{-1} peak seemed to have increased initially (oxygen exposure from 0.4 to ~ 2.7 L), and then decreased (from ~ 2.7 to 3.3 L). The 444-cm^{-1} peak seemed to have emerged for 2.7-L oxygen exposure, and its existence was clearly observed for 3.3 L. For the oxygen exposure of 3.6 L [corresponding to the (3×1) pattern], the 380-cm^{-1} peak virtually disappeared and only the 444-cm^{-1} peak with the FWHM of ~ 105 cm^{-1} was observed. The 444-cm^{-1} peak seemed to have broadened slightly for further oxygen exposures. The FWHM of the 444-cm^{-1} peak for 30-L oxygen exposure (corresponding to the disordered-nickel-oxide pattern) was ~ 115 cm^{-1}. Except for the 444-cm^{-1} peak, in the oxygen exposure region between 3.6 and 30 L, no additional peaks were observed.

In Fig. 2 are shown the effects of thermal treatment on the HRELS spectra of oxygen-covered Ni(110) surfaces. The dotted curve of Fig. 2(a) shows the HRELS spectrum of the Ni(110) surface exposed at 300 K to 0.96-L oxygen. This spectrum has already been shown in Fig. 1, and the energy-loss peaks are at 380 and 480 cm^{-1}. For this surface, the LEED (2×1) pattern has been observed as described in Sec. III A. The solid curve of Fig. 2(a) shows the HRELS spectrum of the surface produced by heating the Ni(110) surface, preexposed to 0.96-L oxygen, at 540 K for 1 min. Only the 380-cm^{-1} peak has been observed (the 480-cm^{-1} peak has disappeared), accompanied by the sharpening of the LEED spots in the (2×1) pattern. The dotted curve of Fig. 2(b) shows the HRELS spectrum of the Ni(110) surface exposed at 300 K to 0.4-L oxygen. The energy-loss peaks are at 380 and 480 cm^{-1}. The initial-(3×1) pattern has been observed (only with difficulty) for this surface as described in Sec. III A. The solid curve of Fig. 2(b) shows the HRELS spectrum of the surface produced by heating the Ni(110) surface, preexposed to 0.4-L oxygen, at 630 K for 1 min. The intensity of the 380-cm^{-1} peak has increased and the 480-cm^{-1} peak diminished; the well-developed initial-(3×1) pattern has been observed.

The dotted curve of Fig. 2(c) shows the HRELS spectrum of the Ni(110) surface exposed at 300 K to 30-L oxygen. The energy-loss peak is at 444 cm^{-1}. The disordered-nickel-oxide pattern has been observed for this surface (Sec. III A). The solid curve of Fig. 2(c) shows the HRELS spectrum of the surface produced by heating the Ni(110) surface, preexposed to 30-L oxygen, at 770 K for 1 min. The observed HRELS peaks are at 400, 544, and 1089 cm^{-1}. For this surface, a much brighter and sharper (2×1) pattern has been observed, in comparison with the (2×1) patterns observed for the Ni(110) surface exposed at 300 K to 0.96-L oxygen and for the surface produced by heating the Ni(110) surface, preexposed to 0.96-L oxygen, at 540 K for 1 min.

The signal intensity was found to be peaked in the specular direction by the rotation of the sample or the analyzer. The intensity of the elastically-scattered electrons from the gas-covered surface was reduced to $\sim\frac{1}{10}$ of that from the clean surface. The off-specular measurement[17] was not made, though attempted, due to the very low signal intensity. The HRELS technique has been applied to oxygen-covered Ni(110) surfaces for the first time in this work, and comparison of the experimental results with those of other investigators cannot be made at present.

C. AES and $\Delta\phi$

Figure 3 shows the change in the Auger peak-height ratio, $H(OKL_{2,3}L_{2,3})/H(NiL_{2,3}VV)$, as the Ni(110) clean surface at 300 K has been exposed to the increasing amount of oxygen. A rapid monotonic increase was observed up to ~1 L. Further oxygen exposure up to ~5 L caused a slow increase. The Auger peak-height ratio was increased rather quickly from ~5 to 30 L, and then slowly from ~30 to 100 L. The Auger peak-height ratio was nearly saturated beyond ~100-L oxygen exposure. These results are in reasonable agreement with those of other investigators.[18,19] The oxygen coverage θ in the saturation region has been measured to be two monolayers (ML) [1 ML$=1.14\times10^{15}$ atoms/cm^2 for Ni(110)], using photoemission (ultraviolet and x ray) and $^{16}O(d,p)^{17}O$ nuclear microanalysis (Norton *et al.*[20]), reflection high-energy-electron diffraction (RHEED) and x-ray emission (Mitchell *et al.*[12]), and LEED and Rutherford backscattering with channeling and blocking (Smeenk *et al.*[13]). The oxygen coverages of oxygen-covered Ni(110) surface can, therefore, be estimated using our data, assuming that the above-mentioned Auger peak-height ratio is proportional to the oxygen coverage (neglecting the effects of the in-depth distribution of oxygen, the es-

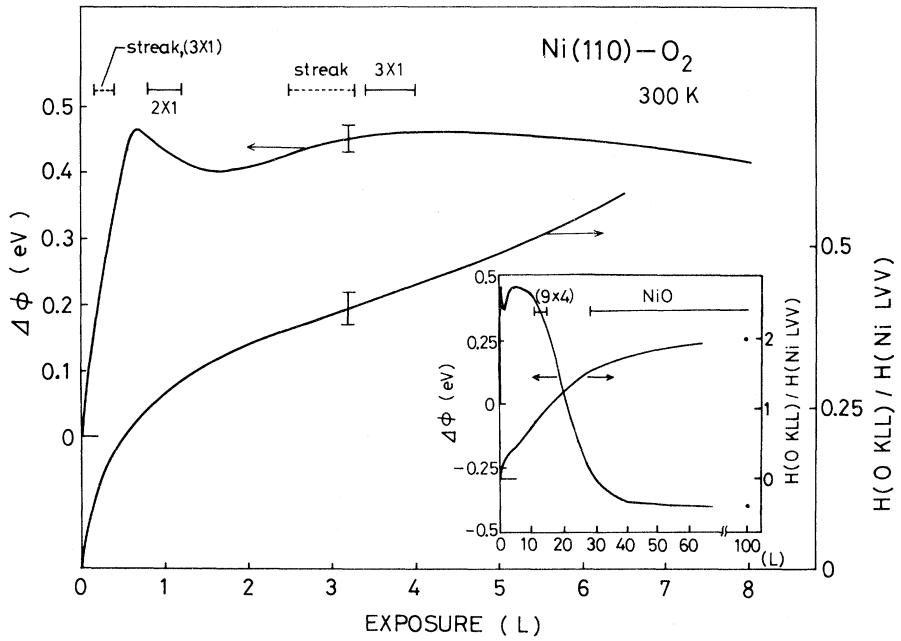

FIG. 3. Work-function change $\Delta\phi$, the Auger peak-height ratio $H(OKL_{2,3}L_{2,3})/H(NiL_{2,3}VV)$, and the observed LEED patterns as a clean Ni(110) surface is exposed at 300 K to the increasing amount of oxygen. Rough estimates of the fractional oxygen coverages are included in the AES results. The results for the high oxygen exposure region are shown in the inset.

cape depth of Auger electrons, etc.) and that the Ni(110) surface exposed to 100-L oxygen corresponds to 2 ML. The oxygen coverages corresponding to the (2×1), (3×1), and (9×4) patterns are ~0.3, 0.4, and 1 ML, respectively (Fig. 3). In spite of the rough estimation, these values are in reasonable agreement with those of other investigators[12,13,20] mentioned above. It is noted, however, that the problem concerning the oxygen coverages has not yet been settled. Germer *et al.*[1,3–5] have considered that the above patterns respectively represent $\frac{1}{2}$, $\frac{2}{3}$, and $\frac{10}{9}$ ML from the oxygen exposure required to produce each pattern.

Also shown in Fig. 3 is the work-function change $\Delta\phi$ as a function of oxygen exposure. The work-function change increased monotonically, in the initial stage of adsorption, up to ~0.6 L ($\Delta\phi_{max}\sim0.46$ eV), then decreased between ~0.6 and 1.6 L [corresponding to the (2×1) pattern], and again increased between ~1.6 and 4.5 L. The work-function change decreased greatly between ~4.5- and 30-L oxygen exposure, and slowly beyond ~30 L. The work-function change corresponding to the (9×4) pattern was ~0.35 eV. The work-function change for 100-L oxygen exposure (corresponding to the disordered-nickel-oxide structure) was -0.4 eV. These results are in reasonable agreement with those of other investigators.[7,19] Demuth and Rhodin[7] have observed the (2×1) LEED pattern at (not after, as in our case) the initial maximum in their $\Delta\phi$ versus exposure curve; however, this difference does not invalidate the discussion later (Sec. IV B). The work function for nickel oxide can be estimated to be 4.6 eV, using the work function change for 100-L oxygen exposure and the work function for Ni(110) (5.04 eV),[21] in fair agreement with that for nickel oxide produced by the oxidation of an Ni film (4.4 eV).[22]

IV. DISCUSSION

A. The Ni(110) disordered-O structure

In the oxygen exposure region below ~0.2 L ($\theta\lesssim0.1$), only the Ni(110)-substrate LEED spots are observed, with their intensities slightly reduced from those of the clean surface. Using HRELS, a single vibrational loss peak at 480 cm^{-1} is observed (Fig. 1). Besides, the monotonic increase in the work-function change $\Delta\phi$ and in the Auger peak-height ratio $H(OKL_{2,3}L_{2,3})/H(NiL_{2,3}VV)$ is observed (Fig. 3).

The LEED results indicate that oxygen is adsorbed in the disordered structure. By comparison with the stretching vibrational energy of gaseous oxygen (O_2: 1555, O_2^+: 1858, and O_2^-: 1145 cm^{-1}),[23] the observed energy-loss peak is attributed to the stretching vibrational excitation of the oxygen atoms adsorbed on the Ni(110) surface. The HRELS, AES, and $\Delta\phi$ results indicate that the oxygen atoms are adsorbed in a single state. The $\Delta\phi$ measurement may indicate that the adsorbed oxygen atoms are negatively charged. The Ni(110) substrate is, by the oxygen adsorption, considered to be unreconstructed from the LEED and $\Delta\phi$ results, in agreement with the results from low-energy ion scattering.[10,11,13]

For HRELS in the specular mode, the incident electrons interact mainly with the long-range dipole field induced by the vibrating "surface molecules" and only vibrational modes with the dipole-moment component perpendicular to the surface are predominantly observed.[24,25] The observed vibrational mode belongs to the totally symmetric representation of the point group of surface molecules ("surface-normal dipole selection rule"). The number of the observed vibrational modes as well as the vibrational energy contain information on the structure of surface molecules.

As described above, we have observed a single HRELS peak at 480 cm^{-1}. The number of the observed vibrational mode indicates that the oxygen atoms are located in the high-symmetry sites. Candidates for the adsorbed site are, therefore, the on-top site, the short-bridge site (midway between two Ni atoms in contact of spacing $d=2.49$ Å), the long-bridge site (another type of two-atom bridging site where the interatomic spacing is $\sqrt{2}d$), and the twofold hollow site (site in the middle of the rectangular mesh). There is no vibrational study on oxycomplexes of nickel which has been reported. Thus, it is somewhat difficult to extract the structural information from the vibrational energy. The oxygen atoms are believed not to be located in the on-top sites. For an oxygen atom in the on-top site, the chemical bond would be shared essentially with one nearest-neighbor nickel atom. According to the crude valence-force-field model, the corresponding stretching vibrational energy is expected to be close to that for the gaseous NiO (615 cm^{-1}),[26] which is substantially higher than the observed vibrational energy (480 cm^{-1}). The stretching vibrational energy $\hbar\omega_B$ expected for an oxygen atom in the bridge site is, if one assumes the sum

of the bond forces to be nearly the same for different sites, given by

$$\hbar\omega_B \sim 615 \left[\left(\frac{1}{2} + \frac{m_{\mathrm{Ni}}}{m_0} \cos^2 \frac{\gamma}{2} \right) \frac{m_0}{m_0 + m_{\mathrm{Ni}}} \right]^{1/2}, \quad (1)$$

where γ is the Ni—O—Ni bond angle, m_0 and m_{Ni} the respective masses of O and Ni.[27] The effective radius of an oxygen atom [absorbed on the Ni(100) surface] has been estimated to be 0.74 Å.[8] Thus, for an oxygen atom in the short-bridge site of the Ni(110) surface, $\gamma = 78°$ and $\hbar\omega_B = 470$ cm^{-1}; for oxygen in the long-bridge site, $\gamma = 125°$ and $\hbar\omega_B = 323$ cm^{-1}. Therefore, the 480-cm^{-1} peak can be attributed to the oxygen atoms in the short-bridge sites. The assumption of the sum of the bond forces being nearly the same for different sites is, to some degree, equivalent to the statement that the desorption energies of oxygen for different sites (which, unfortunately, are not known for the nickel surface) are nearly the same. This assumption has been found to be valid for oxygen-covered W(100) surfaces.[28] The short-bridge site has been favored from the consideration of the orbital hybrid directions for the bonding of an oxygen atom on the Ni(100) surface.[29] Considering the small effective radius of an oxygen atom, the oxygen atoms are believed not to occupy the hollow sites by the argument similar to that for the on-top sites.

From the above discussion, it is proposed that, in the oxygen exposure region below ~0.2 L, the oxygen molecules are dissociatively adsorbed on the Ni(110) surface, at random, in a single state and that the adsorbed oxygen atoms are located in the short-bridge sites of the unreconstructed Ni(110) substrate (simple-addition model). In Fig. 4(a) is shown the proposed structural model of the disordered-O surface. Chemisorption in this oxygen exposure region is associated with strong binding of the adsorbate to the substrate but negligible substrate disruption.[7]

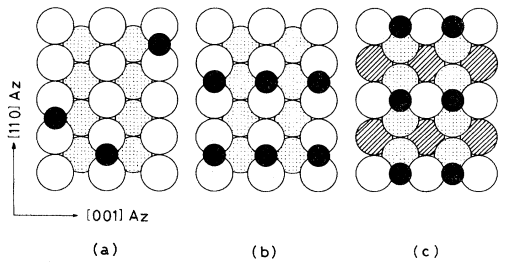

FIG. 4. Structural models of (a) the Ni(110) disordered-O structure, (b) the Ni(110) unreconstructed (2×1)-O structure, and (c) the Ni(110) reconstructed (2×1)-O structure; filled, open, dotted, and hatched circles represent oxygen, Ni first layer, Ni second layer, and Ni third layer, respectively.

B. Surface structure when the LEED (2×1) pattern is observed

In the oxygen exposure region of ~1 L ($\theta \sim 0.3$), the (2×1) LEED pattern is observed, accompanied by the work-function decrease (Fig. 3). Using HRELS, the 380-cm^{-1} peak is observed, in addition to the 480-cm^{-1} peak. The intensity of the 480-cm^{-1} peak is at the maximum (Fig. 1).

The 480-cm^{-1} peak is attributed to the oxygen atoms in the unreconstructed (2×1)-O structure. The local structure of this structure is similar to that of the disordered-O structure described in Sec. IV A. Demuth *et al.*[7,8] have proposed that the oxygen atoms in the (2×1)-O structure are located in the short-bridge sites of the unreconstructed Ni(110) surface from the LEED dynamical calculation. The additional peak at 380 cm^{-1} is attributed to the excitation of the stretching vibration associated with the adsorbed oxygen atoms in a state different from those in the unreconstructed (2×1)-O structure: The main reason for the difference in the stretching vibrational energies for the two kinds of adsorbed states is considered to be the site-dependent chemical-bond effect (in addition, the self-image effect,[30] etc., may be needed to account for the difference). In fact, heating of the Ni(110) surface, preexposed to ~1-L oxygen, at 540 K for 1 min has resulted in the disappearance of the 480-cm^{-1} peak, with the 380-cm^{-1} peak still surviving [Fig. 2(a), Sec. IV D]. The existence of the two adsorbed states of oxygen, when the (2×1) LEED pattern is observed, has clearly been demonstrated for the first time in this work.

The 380-cm^{-1} peak is also associated with the (2×1)-O structure, because its growth coincides with the appearance of the LEED (2×1) pattern. An additional evidence for this statement is that the sharpening of the LEED spots in the (2×1) pattern by the heat treatment mentioned above has been observed (Sec. III B). The (2×1)-O structure associated with the 380-cm^{-1} peak is hereafter called the "reconstructed (2×1)-O structure," from the discussion on the work-function change below. The oxygen atoms in this structure are considered to be disruptively bonded to the substrate lattice accompanied with distortion of the lattice.[7]

As the oxygen exposure is increased from 0.96 to 2 L, the intensity of the 380-cm^{-1} peak is slightly increased (Fig. 1), whereas the intensity of the LEED spots in the (2×1) pattern is decreased (Fig. 3). This would appear contradictory to the assignment that the 380-cm^{-1} peak is related to the (2×1)-O structure. However, it should be remembered that the LEED pattern reflects the long-range periodic structure of the surface, whereas HRELS is sensitive to the local structure. By increasing the oxygen exposure from 0.96 to 2 L, the oxygen atoms would be adsorbed at sites related to the 380-cm^{-1} peak, but by which the long-range periodic structure is destroyed.

From the HRELS peak intensities and AES results for 0.15- and 0.96-L oxygen exposures, the oxygen coverage, for 0.96-L oxygen exposure, in the unreconstructed (2×1)-O structure is estimated to be of comparable amount with that in the reconstructed (2×1)-O structure (the effective charge associated with the 480-cm^{-1} peak is assumed to be independent of oxygen coverage).

The decrease of the work-function change $\Delta\phi$ in the oxygen exposure region from ~0.6 to 1.6 L is interpreted to indicate that the Ni(110) substrate is reconstructed. Similar decrease in $\Delta\phi$ observed for an Ni(100) surface has also been attributed to the reconstruction process.[31] Combining the $\Delta\phi$ and HRELS results (Fig. 1), it can be stated, with the increase of the oxygen exposure from 0.96 to 1.6 L, that the number of the reconstructed (2×1) units is increased and that the number of the unreconstructed (2×1) units decreased. It is noted that the minimum in $\Delta\phi$ near 1.6-L oxygen exposure is due to the combined effect of the decrease in the dipole moment per adsorbed oxygen and the increase in the oxygen coverage; the dipole moment per oxygen, estimated from $\Delta\phi[H(OKL_{2,3}L_{2,3})/H(NiL_{2,3}VV)]$, is monotonically decreased from the oxygen exposure of ~0.6 to 5 L, in agreement with the result of Benndorf *et al.*[19]

The reconstruction of the Ni(110) substrate would occur such that every other Ni[001] row is absent.[1] Thus, from the comparison of the observed vibrational energy (380 cm^{-1}) with the crude valence-force-field model calculation (323 cm^{-1}) described above, the oxygen atoms in the reconstructed (2×1)-O structure are considered to be located inbetween the Ni atoms in the remaining [001] rows. It is noted that the local geometry of this structure is similar to that of the long-bridge site on the unreconstructed surface. Verheij *et al.*[10,11] have proposed a similar model, from the study using low-energy Ar^+ and Ne^+ ion scattering, in which the oxygen atoms lie in or close to the [001] rows of the reconstructed Ni(110) surface. Concerning the location of the oxygen atoms, Germer and MacRae[1] have proposed that they occupy the sites of the absent nickel atoms of the reconstructed Ni(110) surface [which are similar to the twofold hollow sites of the unreconstructed Ni(110) surface]. This model is considered not to be adequate from the valence-force-field model described above.

As discussed above, we have attributed the 480- and 380-cm^{-1} peaks to the unreconstructed and reconstructed (2×1)-O structures, respectively. Other possible explanations are (1) the 480-cm^{-1} peak is associated with the disordered-O structure and (2) the oxygen atoms associated with both peaks are adsorbed at the short-bridge sites of the unreconstructed Ni(110) surface, the energy shift being due to a change in binding energy and bond length.[32] The former would be dismissed considering the LEED dynamical study of Demuth *et al.*,[7,8] and the latter by the work-function decrease discussed above and by the observation of the 380-cm^{-1} peak attributed to the reconstructed (2×1)-O structure for the Ni(110) (2×1)-O surfaces produced by high-temperature heating (Sec. IV D).

From the above discussion it is proposed that, in the oxygen exposure region of ~1 L, the oxygen molecules are dissociatively adsorbed in two structures, i.e., in the unreconstructed and reconstructed (2×1)-O structures. The oxygen atoms in the unreconstructed (2×1)-O structure are considered to be located in the short-bridge sites of the unreconstructed Ni(110) surface [Fig. 4(b)] and the oxygen atoms in the reconstructed (2×1)-O structure in the bridge sites along the Ni[001] rows of the reconstructed Ni(110) surface [Fig. 4(c)].

Some of the limitations in the analyses of the present and previous sections are summarized. The HRELS results in the specular mode are interpreted in terms of the dipole scattering mechanism. The contribution of the short-range scattering mechanisms, although expected to be very small,[17] has to be examined. Simple valence-force-field model has been employed for the structural determination, and this treatment requires a theoretical verification. Andersson[32] has observed the HRELS peaks at 428 and 319 cm^{-1} attributed, respectively, to the vibration of oxygen atoms in the fourfold hollow sites for the Ni(100) $p(2\times2)$-O and Ni(100) $c(2\times2)$-O structures; Ibach and Bruchmann[33] have

observed the HRELS peak at 580 cm^{-1} attributed to oxygen atoms in the threefold hollow sites for the Ni(111) $p(2\times2)$-O and Ni(111) $(\sqrt{3}\times\sqrt{3})R30°$ -O structures. It is difficult, however, to correlate the stretching vibrational energies observed for Ni(110), Ni(100), and Ni(111) surfaces with adsorbed sites by a simple valence-force-field model; e.g., the nickel-oxygen stretching vibrational energy for the threefold hollow site is very close to that for the gaseous NiO and is considerably larger than those for the fourfold hollow and twofold bridge sites. It is emphasized that the stretching vibrational energy depends on the force constant, which is dependent on the curvature of the adsorption potential well.

C. The disordered-nickel-oxide structure, the Ni(110) (9×4) structure, etc.

Beyond ~30-L oxygen exposure ($\theta\sim1.6-2$), the diffuse substrate LEED spots with a bright background are observed. Using HRELS, a single energy-loss peak at 444 cm^{-1} with the FWHM of ~115 cm^{-1} is observed. The observed work-function change $\Delta\phi$ is $-(0.3\sim0.4)$ eV. The LEED results indicate that the sample surface is disordered. The $\Delta\phi$ results (discussed in Sec. III C) together with the LEED results indicate that the disordered-nickel-oxide structure is formed on the Ni(110) surface. This identification is in agreement with those of other investigators.[1,2,5,7,11–13,18–20] Using RHEED, the size of a nickel-oxide crystallite has been estimated to be less than 10 Å.[12] The nickel-oxide layer is, as discussed in Sec. III C, of about one full oxide layer unit-cell thickness. The HRELS peak at 444 cm^{-1} is attributed to the vibration of the sublattices of the nickel-oxide crystallite against each other (which produces an oscillating dipole moment by the long-range Coulomb field in nickel oxide). The nickel (or oxygen) ion sublattices in different crystallites can vibrate in phase, and can be detected by HRELS in the specular mode. The large FWHM (~115 cm^{-1}) of the 444-cm^{-1} peak is attributed mainly to the inhomogeneity in crystallite shape and size. Other possible mechanisms are the coupling of substrate phonon modes to the vibration associated with nickel oxide,[34] the decaying image,[35] the resonance broadening,[36] etc. The infrared absorption experiments of ionic microcrystals sized (NiO, MgO, etc.) sized ~100–1000 Å have been performed by a number of investigators.[37] On the other hand, the lattice dynamical calculations of ionic microcrystals sized ~10–20 Å have been performed by several investigators.[38] Both experiments and calculations indicate that the infrared absorption related to the surface vibrational modes of ionic microcrystals mainly occurs in the energy region between the energy $\hbar\omega_L$ of the long-wavelength bulk longitudinal-optical phonon and the energy $\hbar\omega_T$ of the long-wavelength bulk transverse-optical phonon. Although the effects of the nickel substrate, etc., have to be considered, it is interesting to note that the 444-cm^{-1} peak in the present work is located between $\hbar\omega_L$ (577 cm^{-1}) and $\hbar\omega_T$ (387 cm^{-1}) of NiO.[39]

In the oxygen exposure region of ~13 L ($\theta\sim1$), the (9×4) LEED pattern is observed. The HRELS results are similar to those of the disordered-nickel-oxide structure (Fig. 1). The work-function change $\Delta\phi$ is ~0.35 eV (Fig. 3). The HRELS and $\Delta\phi$ results are considered to indicate that the nickel-oxide patches (crystallites) are formed on the nickel surface. For the (9×4) structure, May and Germer[5] have proposed a two-dimensional pseudo-oxide model in which an oxide monolayer very like a (100) plane of NiO except smaller by about 5% is formed. The present experimental results are compatible with this model. The poor resolution of the LEED spots in the (9×4) pattern and the similarity of the HRELS spectra corresponding to the (9×4) and disordered-nickel-oxide structure are interpreted to indicate that the pseudo-oxide layer is composed of the nickel-oxide patches of limited extent.

In the oxygen exposure region between 3.4 and 4 L ($\theta\sim0.4$), the (3×1) LEED pattern is observed. As in the case of the (2×1) pattern, the fractional order spots in the (3×1) pattern have an intensity comparable to that of the spots from the nickel substrates. The HRELS spectra (Fig. 1) in this oxygen exposure region is very similar to those of the (9×4) and disordered-nickel-oxide structures. The work-function change per adsorbed oxygen is, as discussed in Sec. IV B, monotonically decreased from the oxygen exposure of ~0.6 to 5 L. The LEED and $\Delta\phi$ results are interpreted to indicate that, as in the case of the reconstructed (2×1)-O structure, the substrate is reconstructed. The HRELS results indicate that the nickel oxide patches are formed when the (3×1) LEED pattern is observed, in agreement with the proposal by Smeenk *et al.*[13] from the study using Rutherford backscattering. Germer and MacRae[1] have proposed a model for the (3×1)-O structure in which the Ni[001] rows are formed on top of the Ni(110)

surface separated by three times the original spacing along the [110] direction and in which the oxygen atoms occupy the positions of the absent nickel atoms. This model seems not to be compatible with the HRELS results, considering the simple valence-force-field model discussed in Sec. IV A.

It is difficult to understand why the spectral shape, especially the intensities, of the 444-cm^{-1} peaks for the (3×1)-O, (9×4), and disordered-nickel-oxide structures are nearly the same, although the corresponding oxygen coverages are respectively ~0.4, 1, and 2. This is attributed to a combination of several effects: (1) The intensity of the 444-cm^{-1} peak may give only a rough measure of the amount of nickel oxide due to the angular broadening of the electron beam reflected from the disordered-nickel-oxide patches (whose amount is the largest for the disordered-nickel-oxide structure)[14]; (2) HRELS in the specular mode is sensitive to the long-range dipole field produced outside the crystal,[24,25] etc. The FWHM of the 444-cm^{-1} peak for the (3×1)-O structure is ~105 cm^{-1}, and for the disordered-nickel-oxide ~115 cm^{-1}. The fact that the FWHM of the 444-cm^{-1} peaks are nearly the same for the (3×1)-O, (9×4), and disordered-nickel-oxide structures would be interpreted to indicate that the inhomogeneity in the shape and size of the nickel-oxide patches are of similar extent in these three structures.

In the oxygen exposure region of ~0.4 L ($\theta\sim0.2$), the initial-(3×1) pattern is observed (but with difficulty). Heating of the Ni(110) surface, preexposed to ~0.4-L oxygen, at 630 K for 1 min has resulted in the decay of the HRELS peak at 480 cm^{-1} and in the enhancement of the 380-cm^{-1} peak [Fig. 2(b)]. This change has been accompanied by the well-developed initial-(3×1) pattern (Sec. III B). Therefore, as in the case of the (2×1)-O structure, the initial-(3×1)-O structure can be related to the HRELS peaks at 480 and 380 cm^{-1}; the 480-cm^{-1} peak is associated with the unreconstructed initial-(3×1)-O structure and the 380-cm^{-1} peak the reconstructed initial-(3×1)-O structure. The local structure of the unreconstructed initial-(3×1)-O structure is considered to be similar to that of the disordered-O structure. The reconstructed initial-(3×1)-O structure would be similar to the reconstructed (2×1)-O structure, except that the Ni[001] rows on top of the nickel surface are separated by three times the original spacing along the [110] direction.[1]

In the oxygen exposure region from ~2.5 to 3.3 L ($\theta\sim0.4$), the LEED streaks are observed. The HRELS results indicate that the 444-cm^{-1} peak emerges accompanied by the decay of the 380-cm^{-1} peak. In agreement with Germer *et al.*,[4] these results can be understood in terms of the structural composites of gradually increasing oxygen content which are made up of the (2×1) (mostly reconstructed) and (3×1) units; the structural composites, at a particular coverage, have repeating atomic sequences of different lengths but of similar oxygen concentration. In the same way, the LEED streaks observed in the oxygen exposure region between ~0.2 and 0.4 L ($\theta\sim0.2$) could be explained in terms of the structural composites composed of the substrate (1×1), initial-(3×1), or (2×1) units. Germer *et al.*[4] have observed, at 300 K, the well-developed initial-(3×1) pattern and the LEED streaks; the LEED streaks have been observed before and after the initial-(3×1) pattern is seen. The streaks before the initial-(3×1) pattern have been attributed to the structural composites composed of the substrate (1×1) and initial-(3×1) units and the streaks after the initial-(3×1) pattern to the structural composites composed of the initial-(3×1) and (2×1) units.

Of special interest is the shift of the HRELS peak at 380 cm^{-1} (for 0.4-L oxygen exposure) by 20 to 400 cm^{-1} for 3.3 L. This clearly points to the occurrence of a collective behavior of the adsorbed oxygen atoms. The energy shift is caused by a combination of several effects: the dipole-dipole interaction,[40] the through-substrate vibrational coupling,[41] the local electric-field modification brought about by other adsorbates,[42] etc.

D. Ni(110) (2×1)-O surfaces produced by high-temperature heating

For the Ni(110) (2×1)-O surface produced by room-temperature adsorption of oxygen on the Ni(110) surface, two HRELS peaks at 480 and 380 cm^{-1} are observed. This has been interpreted to indicate that the oxygen atoms are adsorbed in two structures (Sec. IV B). The 480-cm^{-1} peak is associated with the unreconstructed (2×1)-O structure; the 380-cm^{-1} peak the reconstructed (2×1)-O structure.

For the Ni(110) (2×1)-O surface produced by heating the Ni(110) surface, preexposed to 0.96-L oxygen at 540 K for 1 min, only the HRELS peak at 380 cm^{-1} is observed; the 480-cm^{-1} peak is nonexistent (Sec. III B). This is interpreted to indi-

cate that only the Ni(110) reconstructed (2×1)-O structure is present.[10,11] In addition, most of the oxygen in the Ni(110) unreconstructed (2×1)-O structure must have dissolved just below the nickel surface [some may have participated in the formation of the Ni(110) reconstructed (2×1)-O structure]. Sharpening of the LEED spots in the (2×1) pattern (Sec. III B) is considered to be caused by thermal ordering of the reconstructed (2×1) units.

For the Ni(110) (2×1)-O surface produced by heating the Ni(110) surface, preexposed to 30-L oxygen at 770 K for 1 min, three HRELS peaks are observed at 400, 544, and 1089 cm^{-1} (Sec. III B). The characteristic energy loss at 544 cm^{-1} (±12 cm^{-1}) is between the energy $\hbar\omega_L$ of the long-wavelength bulk longitudinal-optical phonon of NiO (577 cm^{-1})[39] and the energy $\hbar\omega_s$ of the Fuchs-Kliewer optical surface phonon[43] of a semi-infinite NiO crystal; the latter being calculated to be 534 cm^{-1} by the relation $\hbar\omega_s=[(\epsilon_0+1)/(\epsilon_\infty+1)]^{1/2}\hbar\omega_T$, where ϵ_0 is the static dielectric constant (11.75),[44] ϵ_∞ the high-frequency dielectric constant (5.7),[44] and $\hbar\omega_T$ the energy of the long-wavelength bulk transverse-optical phonon (387 cm^{-1})[39] of NiO. Therefore, referring to the calculation on the optical phonon of an ionic crystal slab placed between two media of different dielectric constants,[45] the 544- and 1089-cm^{-1} peaks are attributed, respectively, to the single and double excitations of the optical surface phonon in the upper branch for nickel oxide formed on the nickel surface. Precisely, the calculations[43,45] predict that, for the present experimental condition (the wave number $k_{||}$ of the phonon detectable by the analyzer $\lesssim10^{-2}$ $Å^{-1}$ and thickness d of the nickel-oxide layer ~4 Å,[13] i.e., $k_{||}d<<2$), the measured characteristic energy loss should be almost equal to the energy $\hbar\omega_L$ rather than to $\hbar\omega_s$, which is contrary to the above results. The reason is attributed to the structural effect of the nickel-oxide layer (discussed below) which causes the deviation of the dielectric constants of the layer from the bulk values. It is noted that, for NiO(100) grown on the Ni(100) surface at 670–870 K under the oxygen pressure of $\sim3\times10^{-6}$ Torr (the thickness of the nickel-oxide layer is not reported, and is estimated to be $\sim30-100$ Å),[12,46] multiple-loss spectra with spacing 544 cm^{-1} (±121 cm^{-1}) attributed to the excitation of the optical surface phonon have been observed.[47] The existence of the nickel-oxide layer for the present surface has clearly been shown by HRELS which is sensitive to the local structure of the surface: the existence cannot be expected simply by observing the well-developed LEED (2×1) pattern. That the nickel oxide is in the form of patches and does not cover the surface in a uniform layer is evidenced by the lack of the diffraction spots associated with nickel oxide (Sec. III B). The size of the nickel-oxide patches, formed by heating an Ni(110) crystal at 770 K in a relatively high oxygen pressure (e.g., 1×10^{-6} Torr) has been estimated to be about 25 Å from the geometrical size of the observed diffraction spots of nickel oxide.[1] The HRELS peak at 400 cm^{-1} [Fig. 2(c)] can be correlated with the observation of the LEED (2×1) pattern. The origin of the 400-cm^{-1} peak is thought to be the same as that of the 380-cm^{-1} peak discussed above, i.e., the existence of the Ni(110) reconstructed (2×1)-O structure[10,11]; the 20-cm^{-1} shift for the present surface is attributed to the collective behavior (Sec. IV C) induced by the existence of nickel-oxide patches. The Ni(110) reconstructed (2×1)-O structure and nickel-oxide patches are considered to coexist in the superficial region of the crystal, because in the specular mode HRELS, primary electrons interact predominantly with the long-range dipole field produced outside the crystal.[24,25] The well-developed LEED (2×1) pattern is caused by the well-developed Ni(110) reconstructed (2×1)-O structure on the surface. Finally, it is noted that the existence of the oxygen atoms which have dissolved below the nickel surface is expected: Smeenk *et al.*[13] have found, using Rutherford backscattering, for the surface produced by heating the Ni(110) surface, preexposed to 70-L oxygen at 775 K (very similar to the present surface), that the thickness of the oxygen-dissolved layer is of the order of 35 Å and that the oxygen atoms displace nickel atoms from their lattice positions.

V. CONCLUSION

The structures of oxygen-covered Ni(110) surfaces have been studied at 300 K using the *in situ* combination of the LEED, HRELS, AES, and $\Delta\phi$ techniques. The proposed structural models are summarized below.

(1) Oxygen exposure below ~0.2 *L* ($\theta\lesssim0.1$). The disordered-O structure is formed; the adsorbed oxygen atoms are located in the short-bridge sites of the unreconstructed Ni(110) surface [Fig. 4(a)].

(2) Oxygen exposure between ~0.2 *and 0.4 L* ($\theta\sim0.2$). The adsorbed structures formed are of the disordered-O structure, the initial-(3×1)-O

structure, and the structural composites composed of the substrate (1×1), initial-(3×1), or (2×1) units. The initial-(3×1)-O structure is divided into the unreconstructed and reconstructed initial-(3×1)-O structures. The local structure of the unreconstructed initial-(3×1)-O structure is similar to that of the disordered-O structure. The reconstructed initial-(3×1)-O structure is similar to the reconstructed (2×1)-O structure described below, except that the Ni[001] rows on top of the nickel surface are separated by three times the original spacing along the [110] direction.

(3) Oxygen exposure between ~0.8 and 1.2 L ($\theta\sim0.3$). Both the unreconstructed and reconstructed (2×1)-O structures are existent. The local structure of the unreconstructed (2×1)-O structure is similar to that of the disordered-O structure [Fig. 4(b)]. The oxygen atoms in the reconstructed (2×1)-O structure are located in the bridge sites along the Ni[001] rows of the reconstructed Ni(110) surface [Fig. 4(c)].

(4) Oxygen exposure between ~2.5 and 3.3 L ($\theta\sim0.4$). The structural composites composed of the reconstructed (2×1) and (3×1) units are present. A small amount of oxygen atoms is in the unreconstructed (2×1)-O structure.

(5) Oxygen exposure between ~3.4 and 4 L ($\theta\sim0.4$). The (3×1)-O structure composed of the nickel-oxide patches is formed.

(6) Oxygen exposure of ~13 L ($\theta\sim1$). The two-dimensional pseudo-oxide composed of the nickel-oxide patches is formed.

(7) Oxygen exposure beyond ~30 L ($\theta\sim1.6-2$). The disordered-nickel-oxide structure composed of the nickel-oxide crystallites is formed.

The Ni(110) (2×1)-O surfaces produced by high-temperature heating have been studied. For the surface produced by room-temperature adsorption of oxygen, followed by high-temperature heating, the oxygen atoms exist in the Ni(110) reconstructed (2×1)-O structure with some oxygen dissolved just below the nickel surface. For the surface produced by exposure of the Ni(110) surface to a large amount of oxygen, followed by high-temperature heating, the oxygen atoms exist in the Ni(110) reconstructed (2×1)-O structure and in nickel-oxide patches with some oxygen dissolved in the selvage region of the nickel substrate.

The present paper has illustrated an application of the *in situ* multitechnique apparatus (LEED, HRELS, AES, and $\Delta\phi$) to the qualitative understanding of complicated surface structures. The correlation of the LEED and HRELS results has been shown to be of great importance for the elucidation of the surface structures. The HRELS measurements have been performed in the specular mode. A further study in the off-specular mode using an advanced electron spectrometer with high electron-beam intensity is expected to give an additional insight into the surface structures. Theoretical studies on surface vibration and experimental studies by the use of angle-resolved photoemission (ultraviolet as well as x ray), extended x-ray absorption fine structure (EXAFS), etc., of oxygen-covered Ni(110) surfaces are greatly anticipated.

ACKNOWLEDGMENT

This research was supported in part by the Grants-in-Aid for Scientific Research from the Ministry of Education and from Toray Science Foundation.

[1]L. H. Germer and A. U. MacRae, J. Appl. Phys. 33, 2923 (1962).
[2]R. L. Park and H. E. Farnsworth, J. Appl. Phys. 35, 2220 (1964).
[3]A. U. MacRae, Surf. Sci. 1, 319 (1964).
[4]L. H. Germer, J. W. May, and R. J. Szostak, Surf. Sci. 7, 430 (1967).
[5]J. W. May and L. H. Germer, Surf. Sci. 11, 443 (1968).
[6]G. E. Becker and H. D. Hagstrum, Surf. Sci. 30, 505 (1972).
[7]J. E. Demuth and T. N. Rhodin, Surf. Sci. 45, 249 (1974); Jpn. J. Appl. Phys. Suppl. 2, 167 (1974).
[8]P. M. Marcus, J. E. Demuth, and D. W. Jepsen, Surf. Sci. 53, 501 (1975).
[9]J. E. Demuth, J. Colloid Interface Sci. 58, 184 (1977).
[10]L. K. Verheij, J. A. Van den Berg, and D. G. Armour, Surf. Sci. 84, 408 (1979).
[11]J. A. Van den Berg, L. K. Verheij, and D. G. Armour, Surf. Sci. 91, 218 (1980).
[12]D. F. Mitchell, P. B. Sewell, and M. Cohen, Surf. Sci. 69, 310 (1977).
[13]R. G. Smeenk, R. M. Tromp, J. F. Van den Veen, and F. W. Saris, Surf. Sci. 95, 156 (1980).
[14]H. Froitzheim, in *Electron Spectroscopy for Surface Analysis*, edited by H. Ibach (Springer, Berlin, 1977), p. 205.
[15]The location of the Bayard-Alpert ion gauge was

modified from the previous one (Ref. 16) for the accurate measurement of the pressure in the high-resolution spectrometer chamber.
[16]M. Nishijima, S. Masuda, Y. Sakisaka, and M. Onchi, Surf. Sci. 107, 31 (1981).
[17]W. Ho, R. F. Willis, and E. W. Plummer, Phys. Rev. Lett. 40, 1463 (1978).
[18]K. H. Rieder, Appl. Surf. Sci. 2, 74 (1978).
[19]C. Benndorf, B. Egert, C. Nöbl, H. Seidel, and F. Thieme, Surf. Sci. 92, 636 (1980).
[20]P. R. Norton, R. L. Tapping, and J. W. Goodale, Surf. Sci. 65, 13 (1977).
[21]B. G. Baker, B. B. Johnson, and G. L. C. Maire, Surf. Sci. 24, 572 (1971).
[22]H. D. Hagstrum and G. E. Becker, Proc. R. Soc. London A331, 395 (1971).
[23]R. D. Jones, D. A. Summerville, and F. Basolo, Chem. Rev. 79, 139 (1979).
[24]E. Evans and D. L. Mills, Phys. Rev. B 5, 4126 (1972).
[25]D.Šokčević, Z. Lenac, R. Brako, and M. Sŭnjíc, Z. Phys. B 28, 273 (1977).
[26]B. Rosen, Nature 156, 570 (1945).
[27]G. Herzberg, *Molecular Spectra and Molecular Structure II. Infrared and Raman Spectra of Polyatomic Molecules* (Van Nostrand, Princeton, 1945).
[28]H. Froitzheim, H. Ibach, and S. Lehwald, Phys. Rev. B 14, 1362 (1976).
[29]K. A. R. Mitchell, Surf. Sci. 92, 79 (1980).
[30]A. A. Lucas and G. D. Mahan, in Proceedings of the International Conference on Vibrations in Adsorbed Layers, Jülich, 1978 (unpublished), p. 1.
[31]K. Akimoto, Y. Sakisaka, M. Nishijima, and M. Onchi, Surf. Sci. 82, 349 (1979).
[32]S. Andersson, Solid State Commun. 20, 229 (1976).
[33]H. Ibach and D. Bruchmann, Phys. Rev. Lett. 44, 36 (1980).
[34]T. B. Grimley, Proc. Phys. Soc. London 79, 1203 (1962).
[35]G. P. Brivio and T. B. Grimley, J. Phys. C 10, 2351 (1977).
[36]G. D. Mahan and A. A. Lucas, J. Chem. Phys. 68, 1344 (1978).
[37]C. Pigenet and F. Fievet, Phys. Rev. B 22, 2785 (1980).
[38]T. P. Martin, Phys. Rev. B 7, 3906 (1973).
[39]W. Reichardt, V. Wagner, and W. Kress, J. Phys. C 8, 3955 (1975).
[40]M. Scheffler, Surf. Sci. 81, 562 (1979).
[41]M. Moskovits and J. E. Hulse, Surf. Sci. 78, 397 (1978).
[42]J. G. Roth and M. J. Dignam, Can. J. Chem. 54, 1388 (1976).
[43]K. L. Kliewer and R. Fuchs, Phys. Rev. 144, 495 (1966).
[44]P. J. Gielisse, J. N. Plendl, L. C. Mansur, R. Marshall, S. S. Mitra, R. Mykolajewycz, and A. Smakula, J. Appl. Phys. 36, 2446 (1965).
[45]R. Ruppin and R. Englman, Rep. Prog. Phys. 33, 149 (1970).
[46]M. J. Graham and M. Cohen, J. Electrochem. Soc. 119, 879 (1972).
[47]G. Dalmai-Imelik, J. C. Bertolini, and J. Rousseau, Surf. Sci. 63, 67 (1977).